AN INFUSION-PRESSURE SYSTEM TO DETERMINE HYDRAULIC CONDUCTIVITY OF SOFT BIOLOGICAL TISSUES AND MONITOR CLINICAL INFUSIONS

By

TATIANA LOPEZ NOBREGA

A THESIS PRESENTED TO THE GRADUATE SCHOOL
OF THE UNIVERSITY OF FLORIDA IN PARTIAL FULFILLMENT
OF THE REQUIREMENTS FOR THE DEGREE OF
MASTER OF ENGINEERING

UNIVERSITY OF FLORIDA

2010

To my family

ACKNOWLEDGMENTS

I would like to thank my family for their support and encouragement, Dr. Sarntinoranont for advising me throughout the progression of my research, my committee members Dr. Tran-Son-Tay and Dr. McFetridge, Jung Hwan Kim for his role as surgeon in the animal experiments and all of my colleagues in the Tissue Biomechanics Lab.

TABLE OF CONTENTS

page

LIST OF TABLES

LIST OF FIGURES

Abstract of Thesis Presented to the Graduate School
of the University of Florida in Partial Fulfillment of the
Requirements for the Degree of Master of Engineering

AN INFUSION-PRESSURE SYSTEM TO DETERMINE HYDRAULIC CONDUCTIVITY OF SOFT BIOLOGICAL TISSUES AND MONITOR CLINICAL INFUSIONS

By

Tatiana Lopez Nobrega

December 2010

Chair: Malisa Sarntinoranont
Major: Biomedical Engineering

The optimization of local drug delivery therapies, such as convection-enhanced delivery (CED), is dependent on knowledge of the underlying tissue properties that govern spatial distribution and drug uptake by cells. In the brain CED may be implemented as a treatment for epilepsy, cancer, Parkinson's disease and other neurological disorders. Hydraulic conductivity is a measure of fluid conductance through porous media; this property is essential for developing accurate transport models. Although, in brain models literature values for excised tissue may be implemented, *in vivo* infusion experiments provide a more accurate description of tissue hydraulic conductivity. In this study, an infusion-pressure system was developed to determine the hydraulic conductivity of biological tissue. The system was tested in agarose hydrogel (2%) and hydraulic conductivity was then estimated using Darcy's law. Next, *in vivo* experiments were performed to determine the hydraulic conductivity of the caudate putamen (gray matter) and the internal capsule (white matter) in the rat brain. Seven microliters of Evans Blue dye were infused at 18 μLh^{-1} and real-time infusion pressures were recorded. The steady state pressure values were used to

determine the apparent hydraulic conductivity of white and gray matter regions. The infusion-pressure system can be employed in a clinical setting as a low cost method of monitoring infusions. The system can also be used in *ex vivo* and other *in vivo* studies to determine the hydraulic conductivity of other soft biological tissues.

CHAPTER 1
BACKGROUND INFORMATION

Convection-Enhanced Drug Delivery (CED)

CED is a local or targeted drug delivery method that relies on pressure-driven bulk flow to deliver therapeutic agents. An infusate containing therapeutic agent is continuously injected in the region of interest via a catheter or cannula coupled to an infusion pump. The infusion pump creates a pressure gradient between the infusion site and the surrounding tissue which forces infusate through the extracellular space. CED provides several advantages over traditional drug delivery techniques. Less than 1% of systemically administered drugs penetrate the blood brain barrier (BBB) to reach the targeted brain tissue, CED bypasses the BBB providing a pharmacokinetic advantage over systemic administration (Bobo, R. 1994). In many cases, CED limits the administered dose, avoiding the potential for systemic toxicity. The major disadvantage of CED is its invasive nature; while other limiting factors include heterogeneity of drug distribution, catheter induced tissue damage, backflow of infusate and the potential displacement of infusate to tissues beyond the target region (Bidros, D.S. 2009). Applications of CED include gene therapy in the treatment of Parkinson's disease (Cunningham, J. 2008), delivery of gene therapy and chemotherapy agents in tumors, epilepsy, Alzheimer's disease and movement disorders (Krauze, M. 2009).

Drug distribution, using CED, is effected by many factors including tissue structure and properties, cannula size, interstitial fluid pressure, as well as the selected infusion site, rate and volume. In order to develop accurate computational models of drug distribution or interstitial transport these properties must be well defined (Kim, J.H. 2009). In efforts to optimize CED, researchers have investigated the effects of flow

rate, infusate pressure and tissue properties on drug distribution and uptake (Barry, S.I. 1992, Basser,P.J. 1992, Chen, M.Y. 1999, Zhang, X. 2000). However, hydraulic conductivity remains an inadequately studied property despite its importance in predicting drug distribution and efficacy in targeting specific tissues.

Brain, Cerebrospinal Fluid and the Blood-Brain Barrier

The brain is a very complex organ from a structural and functional perspective. From a macroscopic perspective, the brain is primarily composed of cells, an extracellular matrix, and vascular structures. In vertebrates, the brain is surrounded by the meninges, a tri-layer tissue composed of the dura, arachnoid and pia maters. Cerebrospinal fluid (CSF) is produced by ependymal cells of the choroid plexus at a rate of 500 milliliters per day. It circulates through the brain's interconnected ventricular system as indicated by the arrows in Figure 1-1. Ultimately, the CSF flows through the subarachnoid space where it enters the bloodstream via large veins. CSF is primarily composed of plasma proteins, glucose, amino acids, uric acid, urea, ions (i.e. chloride, sodium, potassium, calcium, magnesium and hydrogen) and lactic acid (Merritt, H.H. and Fremont-Smith F. 1937). Its primary functions are to nourish, support and protect the brain tissue.

The perivascular space above the pia mater provides an inlet for blood vessels. Astrocytes, a type of glial cell, promote the formation of the tight junctions between the cells that comprise the capillary walls in the CNS. These tight junctions, which are not found in other circulatory blood vessels, serve to inhibit the transfer of pathogens, toxins, etc. across the BBB into the tissue by restricting intracellular diffusion of water-soluble drugs and proteins (Rapoport S.I. 1980). The endothelial cells in the capillary

walls restrict diffusion of macromolecules while only permitting diffusion of small hydrophobic molecules such as oxygen and carbon dioxide.

Brain tissue is a saturated porous media and the tissue can be defined as either white or gray matter. From a transport perspective, white matter is anisotropic and is characterized by afferent myelinated fibers with extracellular flow predominantly occurring in the direction parallel to the fibers; while, gray matter can be assumed isotropic as no preferential distribution is observed and infusate distributes uniformly in the radial direction from a point of infusion.

Hydraulic Conductivity

Hydraulic conductivity is a material property that describes the ease with which fluid flows through porous media. Although distribution is highly dependent on hydraulic conductivity, it remains poorly quantified across many areas of study and in particular with respect to biological tissues. Previous studies have used fluid infiltration and compression (confined and unconfined) testing to determine hydraulic conductivity in agarose gels, cartilage, tumor tissue, white matter and other tissues (Johnson, E.M. 1996, Gu, W.Y. 2002, Lee, S. 2009, Weiss, J.A 2004, Gu, W.Y. 1999, Boucher, Y. 1998, Cheng, S. 2005). However, these methods are limited to *ex vivo* experimentation as they are inapplicable to *in vivo* studies. Thus, there is a need for *in vivo* testing of hydraulic conductivity to develop more accurate computational models. However, it remains challenging to perform *in vivo* pressure studies due to the invasive nature of these experiments as well as the difficulties associated with measuring small deviations in pressure while creating a small measurement footprint. In this study, the steady state infusion pressure was used to determine the apparent hydraulic conductivity of 2%

hydrogel as well as gray and white matter as represented by the rat caudate putamen and internal capsule, respectively.

Transport in Porous Media

Flow in porous media has been studied for over a century. In 1856 Henry Darcy, a French engineer, discovered that the flow rate of water through sand was proportional to the pressure gradient and this empirical relationship became the basis for the study of flow through porous media. Darcy's law uses a continuum approach, where the media is assumed to be uniform and flow through individual pores is not quantified, rather fluid flow is quantified from a macroscopic perspective. In this analysis, sources and sinks were not considered as transport between neighboring blood and lymph vessels and the brain tissue is negligible and no sources or sinks exist in agarose gels. The infusion conditions were characterized as a spherical infusion source surrounded by rigid porous media. As a result of the slow infusion rate administered, the rigid porous model proves to be a valid assumption (Morrison, P. 1999, Pishko, G. 2007). Thus, the continuity equation was reduced to:

$$\frac{1}{r^2}\frac{\partial}{\partial r}(r^2 V_r) = 0 \qquad (1\text{-}1)$$

where r is the radial distance from the infusion site and V_r is the radial velocity. Equation 1-1 was integrated and rewritten in tensor form to describe the anisotropic properties of the tissue (Note: tensors are indicated with bold notation).

$$V_r = -\boldsymbol{K}\frac{dP}{dr} \qquad (1\text{-}2)$$

where $\frac{dP}{dr}$ is the hydrostatic pressure gradient in the radial direction and K is the hydraulic conductivity. In the case of hydrogel media, homogeneous isotropic conditions were applied and Equation 1-2 was simplified to its one dimensional form.

Assuming constant porosity and flow, substituting for velocity in terms of volumetric flow rate (Q) and expressing the pressure gradient as a function of radial distance yields,

$$P(r) = \frac{Q}{4\pi rK} \quad (1\text{-}3)$$

Thus, pressure is simply a function of the distance from the infusion site (r), flow rate (Q) and hydraulic conductivity (K). By inspection of Equation 1-3, greater hydraulic conductivity values produce lower pressure values for constant radial distance and flow rate values. Therefore, a less dense media will have a greater hydraulic conductivity and produce a small pressure profile.

Fiber Optic Pressure Transducer

Fiber optic pressure transducers have an extrinsic optical cavity, often referred to as the Fabry-Perot cavity. The cavity interfaces with the optical fiber on one end and a diaphragm on the opposing end. The diaphragm deforms in response to applied pressure in turn changing the cavity length. The cavity itself is sealed at a constant pressure and deviation of the diaphragm due to changes in external pressure result in a change in the cavity length. Thus, there is an inverse relationship between cavity length and pressure such that smaller cavity lengths reflect greater pressure values. The cavity length is determined by transmitting light through the optical fiber and detecting the reflected light. Figure 12 is a schematic representation of a fiber optic pressure transducer (Watson, S. 2006).

Brain Infusion Pressure Experiments

Previous studies have been conducted in which infusion pressures were measured in efforts to control drug delivery, create computational models, determine hydraulic conductivities and characterize infusion methods. Boucher et al. recorded

intratumoral infusion pressure to estimate the hydraulic conductivity of *in vivo* tumor tissue. The pressure at the point-source needle exhibited transients during infusion such that at constant flow rate 0.1 $\mu Lmin^{-1}$ the infusion pressure initially increased rapidly then leveled off and reached a steady value within 25-60 minutes of infusion. Prabhu et al. used a positive pressure infusion system to model the distribution of Evans Blue infusate by administration of 20, 40, 60, 100, 140 and 180 µL at 0.167 and 1.5 $\mu Lmin^{-1}$ via a 25-gauge needle. The infusion pressure profiles were described as initially exhibiting a rise in pressure over the first 2-4 minutes of infusion followed by a rapid decrease in pressure to a plateau value for the remainder of infusion. In efforts to characterize a micro-fluidic probe for CED, Neeves et al. infused 5 µL Evans Blue labeled albumin at constant pressures (35, 70 and 140 kPa) into the caudate putamen. The fluid velocity was measured experimentally and the apparent hydraulic conductivity was determined by applying isotropic conditions to Darcy's Law as previously described. In our study, the goal was to optimize a method to determine *in vivo* hydraulic conductivity of gray and white matter, decrease the time required to reach steady state pressure, reduce the measurement footprint via small diameter infusion cannulas, monitor slight (less than 1 mmHg) infusion pressure variations and remove systemic effects from the determined apparent hydraulic conductivities through thorough investigation of the infusion system.

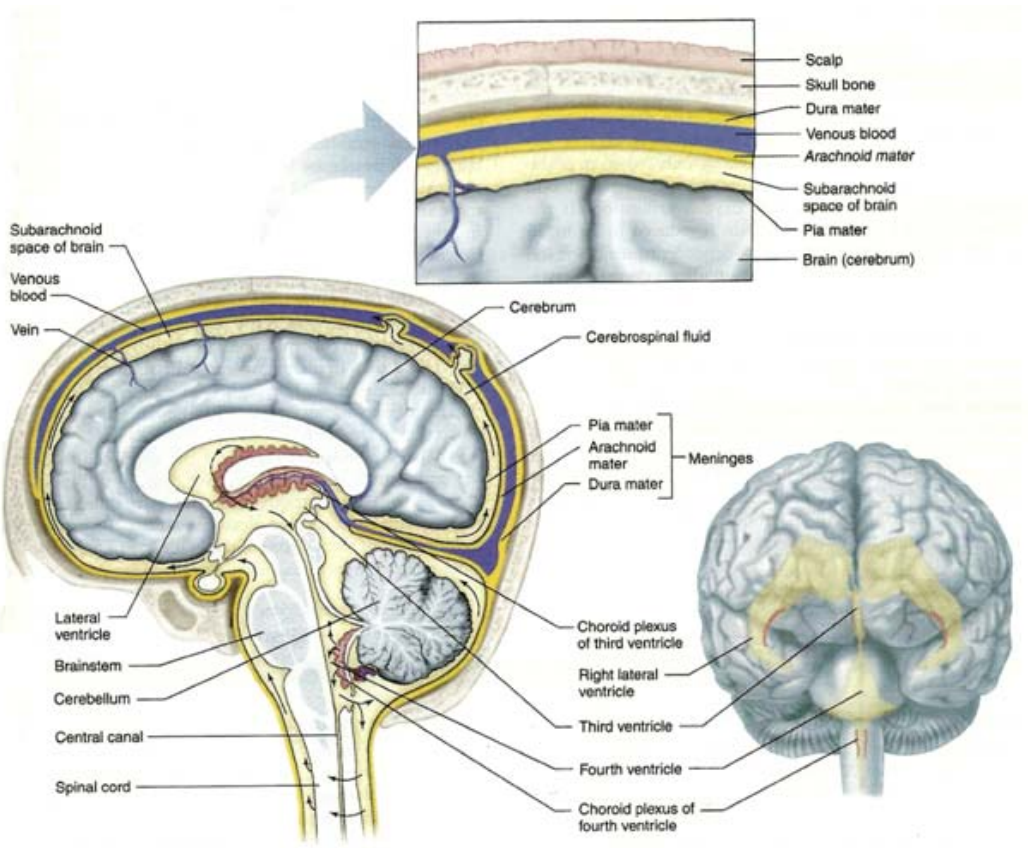

Figure 1-1. Cerebral tissue and fluid structures, arrows indicate CSF flow (Widmaier, E., Raff, H. and Strand, K.T. 2008).

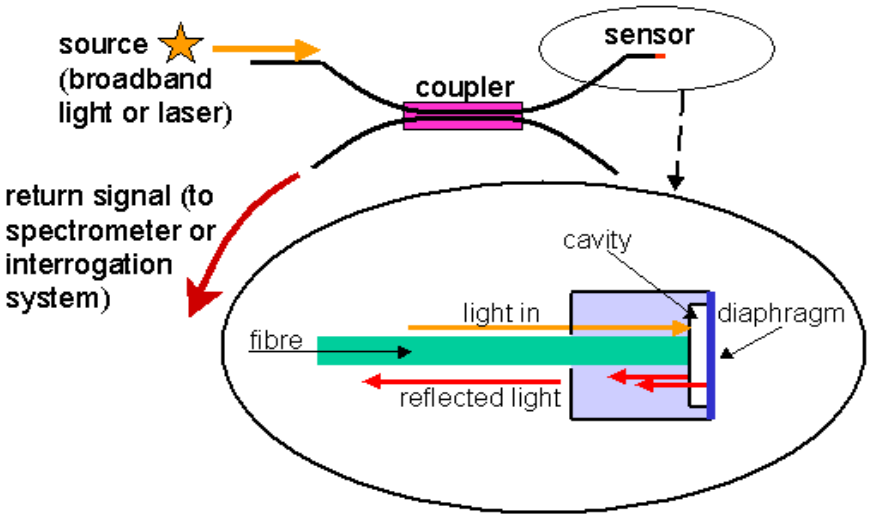

Figure 1-2. Principle of operation of fiber optic pressure transducers (Watson, S. 2006)

CHAPTER 2
MATERIALS AND METHODS

Infusion System

The infusion system consisted of a 100 µl syringe (Hamilton, Reno, NV) coupled to minimally compliant polyaryletheretherketone (PEEK) tubing (Upchurch Scientific, Oak Harbor, WA) of 0.01” inner diameter (ID) and 1/16” outer diameter (OD). A micro-fluidic connector with three ports was used to connect the syringe to a fiber optic pressure transducer as well as the infusion line. The infusion line consisted of the same minimally compliant PEEK tubing coupled, via a reducing union (Valco Instruments, Houston, TX), to the insertion cannula. The cannulas were made by introducing small diameter silica tubing (40 µm ID; 105 µm OD, Polymicro Technologies, Phoenix, AZ) into larger silica tubing (150 µm ID; 360 µm OD, Polymicro Technologies, Phoenix, AZ) and applying adhesive to the joint. The silica assembly was then inserted into PEEK tubing (0.015” ID; 1/16” OD) and glued. Care was taken to minimize the overlap distance during the adhering process and the total volume of the infusion system was calculated to be 0.5 ± 0.025 ml. A screw-drive syringe pump (Cole Parmer, Veron Hills, IL) was used to provide controlled displacement of the syringe plunger during infusion. Figure 2-1 provides a schematic representation of the infusion system and experimental setup. Prior to performing experiments the system was loaded with Evans Blue infusate and purged of air bubbles.

Determining Hydraulic Conductivity under Isotropic and Anisotropic Conditions

Isotropic porous media conditions were applied to 2% hydrogel and gray matter and the apparent hydraulic conductivities were determined analytically using Equation 1-3. The radius of the infusion cavity, r, was assigned a value of 20 µm, the same

dimension as the cannula radius. For the anisotropic case of white matter, a computational model of extracellular transport was created using COMSOL Multiphysics.

Model of Anisotropic Brain Tissue

The tissue was modeled as an eighth of a sphere with a 400 µm radius. The injection site was modeled as a sphere with radius of 20 µm, at the center of the tissue. The model geometry is represented in Figure 2-2 with labeled boundaries. The subdomain was characterized by the mass balance equation (Equation 2-1) where v is the fluid velocity averaged in the representative elementary volume (REV) and φ_B and φ_L are the volumetric flow rates of source and sink terms, respectively. The equation is equal to zero as sources and sinks are negligible in this analysis.

$$\nabla \cdot v = \varphi_B - \varphi_L = 0 \tag{2-1}$$

The velocity term in Equation 2-1, was substituted with Darcy's Law (Equation 1-2), where P and K denote pressure and hydraulic conductivity, respectively (See Equation 2-2).

$$\nabla \cdot v = \nabla \cdot (-\boldsymbol{K} \nabla P) = 0 \tag{2-2}$$

Neumann boundary conditions were applied to symmetric boundaries such that the flow does not penetrate the boundary. Dirichlet boundary conditions were applied to infusion and external boundaries. The average steady state infusion pressure was specified at infusion boundary based on experimental data. A zero pressure condition was applied to the external boundary as the tissue radius is much larger (20r) than the infusion radius and infinite media assumptions were appropriate. Although it is known that white matter is more conductive than gray matter, K in the transverse plane is

unknown. Thus, our approach was to solve for a range of apparent hydraulic conductivities that would encompass the upper and lower bounds. In efforts to find the upper bound of $K_{//}$, the average hydraulic conductivity of gray matter, 2.09E-12 $m^4 N^{-1} s^{-1}$, was used to characterize the transverse plane or $K_{\perp}$. The value of $K_{//}$ was iteratively derived by solving for the volumetric flow rate at the infusion boundary and adjusting $K_{//}$ until the appropriate known volumetric flow rate was obtained. An isotropic solution was determined for each trial and provided the lower bound of $K_{//}$.

Calibration: Fiber Optic Pressure Transducers

The fiber optic pressure transducers used in this study were custom-designed by FISO Technologies (Quebec, CA; Model FOP-MIV-NS663). The design included a stainless steel sleeve which allowed the diaphragm to be recessed from the sensor tip; in turn, protecting the sensor from mechanical damage and facilitating handling. Two small notches where placed at the end of the sleeve to prevent air bubbles from congregating at the recess. The transducers have an operational range of 460 to 1960 mmHg and a resolution of less than 1 mmHg. The FISO UMI4 signal conditioner was used to acquire data at a sampling frequency of 20 Hz.

Static Calibration

The transducers were zeroed under atmospheric conditions. The sensors were then placed in a column of water where the height of the column was varied at 2, 4, 6 and 8 inches. Pressure measurements were recorded for five minutes at each height and the procedure was repeated for six trials.

Dynamic Calibration

The infusion system was assembled as previously described and zeroed under atmospheric conditions. Through the use of a stereotactic frame, the cannula tip was then placed in a beaker of water, 4 mm below the surface. Seven microliters of Evans Blue dye were infused at a rate of 18 μLh^{-1} (0.3 $\mu Lmin^{-1}$). The resulting steady state pressure was used to describe the pressure difference across the infusion system, from the transducer to the cannula tip, under the flow rate condition provided. This value was subtracted from steady state experimental pressures for hydrogel and brain tissue in order to accurately describe the infusion pressure associated with each media.

Hydrogel Experiments

Agarose is a component found in agar which is harvested from red algae. It consists of repeating monomeric units to form a linear polymer. The gel network is made up of double helices formed from left-handed threefold helices stabilized by water molecules within the helix. Hydrogel samples were prepared by weighing 0.8 g of Trevigel 5000 on a balance (Denver Instrument Company, Bohemia, NY) and incorporating 40 mL of deionized water in a beaker. The solution was heated on a hot plate (Barnstead/Thermolyne, Dubuque, IA) until boiling and poured into a 50 mL petri dish. After the hydrogel solidified, the cannula was placed approximately 4 mm below surface level and after a five minute wait period was retracted 0.25 mm to prevent clogging and backflow due to bolus injections. The hydrogel samples were infused with 7 µL of Evan's Blue dye at 18 μLh^{-1} and real-time pressure measurements were obtained. The previously described isotropic porous media model was employed to determine apparent hydraulic conductivity and the experimental values were compared with published values.

Animal Surgery and Experimental Procedure

Experiments were performed on Sprague-Dawley rats (n=6; 270 ± 20 g) per protocols and procedures approved by the University of Florida Institutional Animal Care and Use Committee. The animals were initially anesthetized by 1 mL Xylazine injections and inhalation of 4% isoflurane in 1 $Lmin^{-1}$oxygen. The head was shaved and disinfected with iodide and 70% ethanol. The rats were subsequently placed in a stereotactic frame (David Kopf Instruments Model 900) and anesthesia was reduced to 1% isolfurane in 0.4 L/min oxygen. A mid-sagittal incision was made to the scalp to the level of the skull and the tissue was scrapped and retracted to expose the skull. Two burr holes were made over the coordinates of interest and the areas were cleaned thoroughly using saline. The infusion cannula was then placed in the caudate putamen (AP= 0, ML= -3.5, DV= -4.8) and internal capsule (AP= -1.8, ML= 3, DV= -6.6) as seen in Figure 2-3. The cannula was inserted 0.25 mm deeper and retracted to the final insertion depth indicated after a five minute wait period. Upon retraction, 7 µL of Evans Blue were infused at 18 $\mu Lh^{-1}$and real time infusion pressure data was obtained. Post infusion, the animals were sacrificed by perfusion fixation using 10% buffered formalin. Following decapitation, the brain was removed and stored in 10% buffered formalin. Each brain was then sliced into 400 µm coronal slices using a vibratome (Leica VT1000 A, Bannockburn, IL) and photographed under a microscope. The photos were then examined to confirm the infusion sites were within the targeted regions.

Dynamic Contract Enhanced Magnetic Resonance Imaging Experiments

Dynamic Contrast Enhanced (DCE) Magnetic Resonance Imaging (MRI) experiments were performed in collaboration with Garret Astary and Dr. Thomas Mareci to provide a visual representation of dynamic changes in infusate distribution and the

respective pressure observed. The MR experiments performed utilized the same infusion-pressure system previously described except the infusion PEEK line was replaced with a longer section of the same material in order to place the equipment a safe distance from the magnet. Evans Blue Gd-Albumin was infused at 18 μLh^{-1} in the dorsal (AP = -3.7, ML = -2.2, DV = -2.9) and ventral (AP = -5.0, ML = 4.9, DV = -5.0) CA1 subregion of the hippocampus; the infusion volumes for each region were 8 and 10 µL, respectively. MR experiments were performed using a Bruker Avance imaging console (Bruker NMR Instruments, Billeria, MA) connected to a Magnex Scientific 11.1 Tesla horizontal bore magnet system (Varian, Inc., Magnex Scientific Products, Walnut Creek California). The rat was placed in a custom-built, MR compatible stereotactic frame to eliminate motion during MR imaging. Prior to infusion, three transverse T1-weighted spin-echo images (TR = 330 ms, TE = 9.4 ms, 10 slices at 1 mm thickness, NA = 6, 2.5 cm x 2.5 cm FOV with a 104 x 104 matrix) were acquired to determine the baseline signal in the brain tissue. During infusion of Evans Blue Gd-Albumin the T1-weighted spin-echo images were repeated serially to capture the evolution of the contrast agent distribution and real-time infusion pressure was recorded.

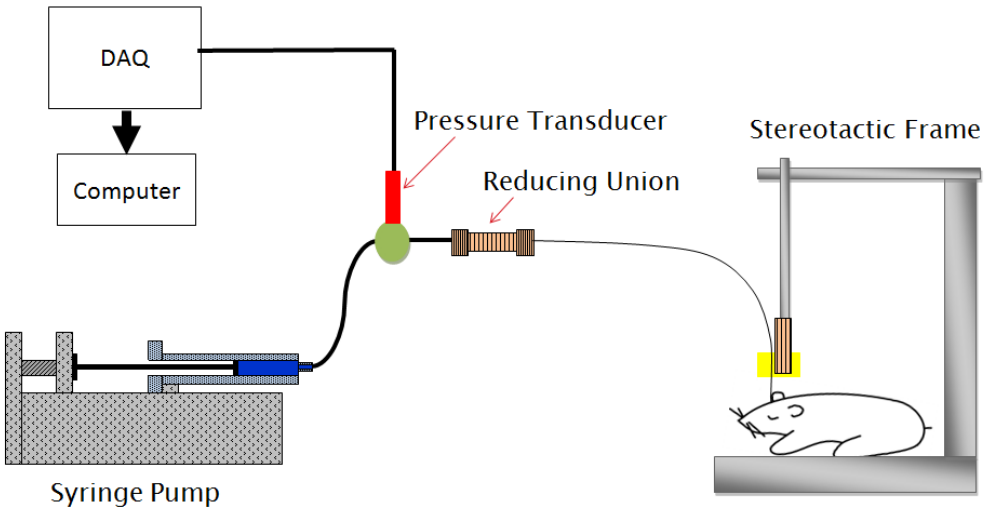

Figure 2-1. Schematic drawing of experimental setup.

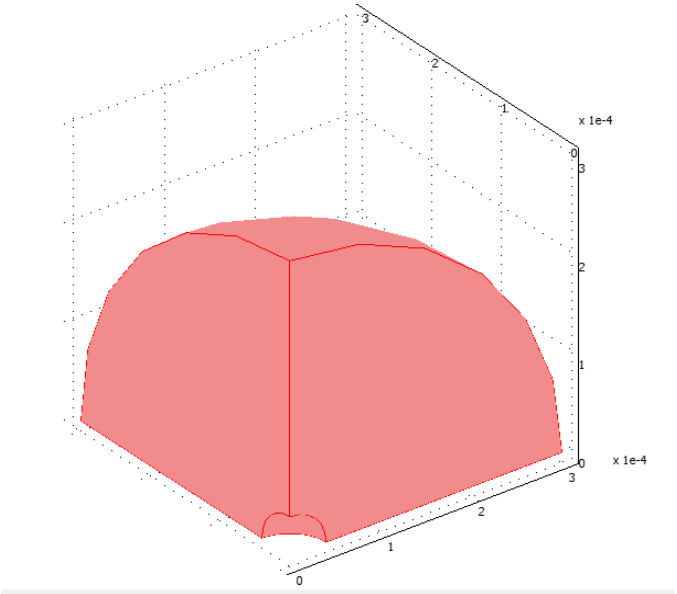

Figure 2-2. Model geometry for infusion into anisotropic tissue.

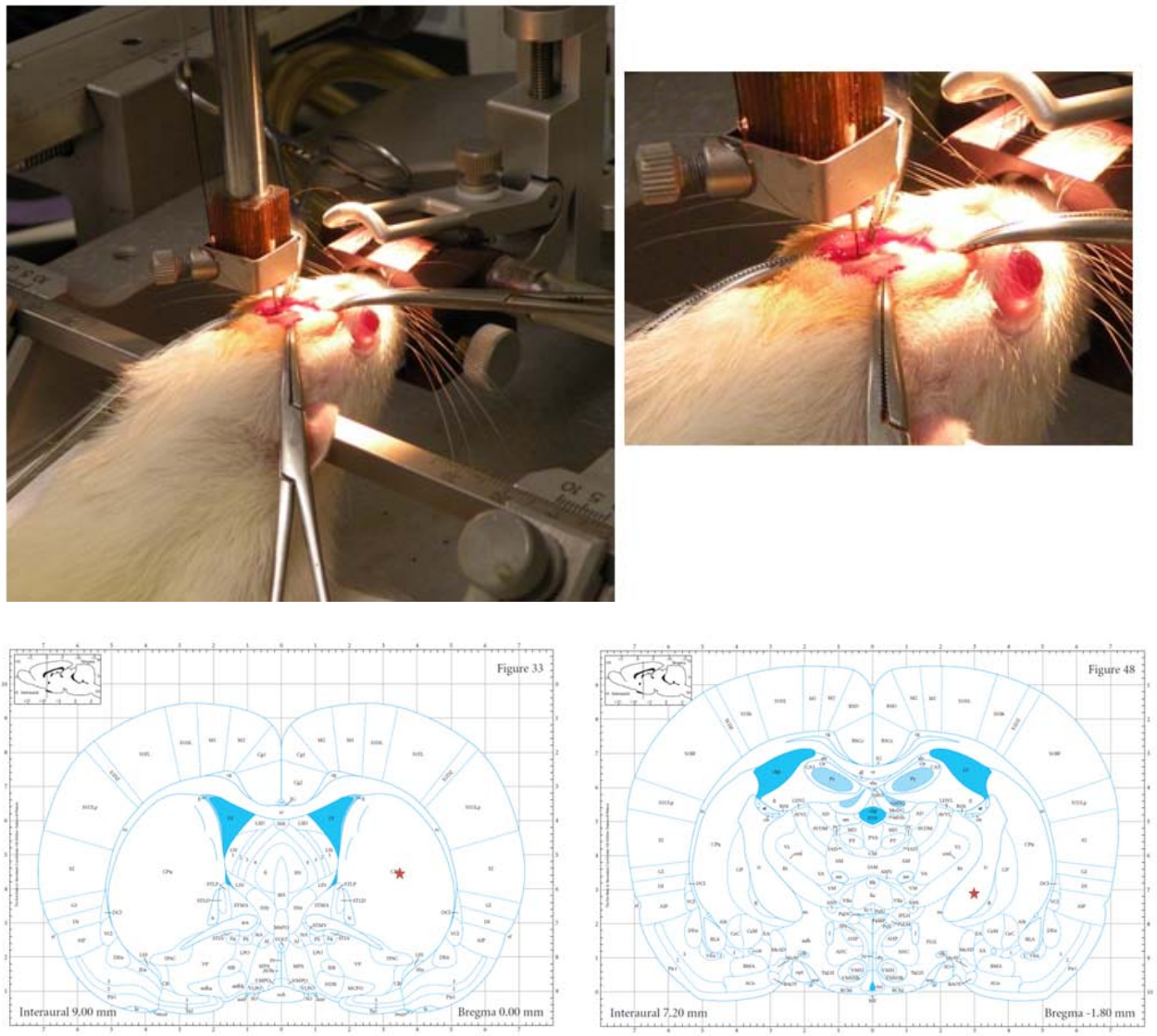

Figure 2-3. (Top Left) Photograph of rat during surgery with cannula placed in brain. (Top Right) Zoomed in view of cannula placement in brain tissue. (Bottom) Figure 33 and Figure 48 of *Paxinos and Watson The Rat Brain* red star indicating targeted caudate putamen (gray matter) and internal capsule (white matter) coordinate, respectively.

CHAPTER 3
RESULTS

Static Calibration

Hydrostatic pressure was recorded over a period of five minutes at each column height for six trials. The theoretical and average pressure values, in mmHg, are graphed in Figure 3-1. Although the experimental values vary from the theoretical values this variation is within ± 1.25 mmHg. Considering the greatest source of error in this experiement was attributed to human error in measuring the water column height, the observed differences in theoretical and experimental pressures were deemed acceptable.

Dynamic Calibration

Infusion pressures, in water, were recorded throughout the infusion period for six trials as seen in Figure 3-2. A transient period is observed at the beginning of data acquisition in which the pressure rapidly increased. This trend is attributed to the development of the boundary layer required to obtain steady state flow conditions as well as the properties of the infusion media. At approximately 200 seconds, the infusion pressure began to stabilize and pressure variations were within ± 3 mmHg. Steady state infusion pressure values were obtained by averaging the data from the start of stabilization to the end of infusion. The hydrostatic pressure due to the cannula tip placement at 4 mm below the surface of the water was subtracted from the steady state pressure values and these average infusion pressures are reported in Table 3-1. The average infusion pressure for the six trials was 52.14 ± 0.63 mmHg. As previously mentioned this pressure represents the systemic pressure drop and was subtracted

from steady state pressure values, in the hydrogel and brain tissue experiments, to determine apparent hydraulic conductivity.

Hydrogel Infusion Data

The 2% hydrogel infusion pressure profiles are shown in Figure 3-3. The steady state pressures vary from 80.27 to 105.06 mmHg; where the average pressure value was 96.08 ± 3.99 mmHg. Trial five demonstrates a typical pressure response when the cannula becomes obstructed or clogged and the infusate does not enter the media immediately. The pressure increased dramatically, approximately 50 mmHg above the average steady state pressure, until a maximum pressure was attained and a bolus injection of infusate was released such that a rapid decrease in pressure was observed followed by pressure stabilization. The remaining trials did not exhibit clogging as was reflected by their smoother pressure profiles. The apparent hydraulic conductivity was calculated using Equation 1-3 and the tabulated values are found in Table 3-2. The average apparent hydraulic conductivity was determined to be 3.61E-12 ± 3.38E-13 $m^4 N^{-1} s^{-1}$.

Caudate Putamen Infusion Data

The pressure profiles generated during infusion into the rat caudate putamen are shown in Figure 3-4. The average steady state infusion pressure was 126.04 ± 4.22 mmHg; where the steady state pressures ranged from 105.32 to 140.34 mmHg. As gray matter is characterized as isotropic, Equation 1-3 was used to determine the apparent hydraulic conductivity of the tissue. The infusion pressures and apparent hydraulic conductivity values are listed in Table 3-3. The average apparent hydraulic conductivities for each trial are graphed in Figure 3-5 and average across the six trials

was 2.09E-12 ± 1.19E-14 $m^4 N^{-1} s^{-1}$. Coronal slices of the final infusate distribution in the caudate putamen for trial 1 are presented in Figure 3-6, where the images progress in the posterior direction. The cannula tract is visible in the third and fourth photos of the second row of Figure 3-6. The infusate penetrated approximately the same distance in the anterior and posterior directions. The infusate is confined within the caudate putamen and does not penetrate surrounding tissue structures.

Internal Capsule Infusion Data

The internal capsule infusion pressure profiles are shown in Figure 3-7. The steady state pressures vary from 84.24 to 141.13 mmHg. The average infusion pressure was 109.18 ± 2.68 mmHg; trial 5 was disregarded when calculating the average pressure and the apparent hydraulic conductivity as this data set exhibited infusate along the cannula tract or backflow. The pressure profile for trial 5 demonstrates a typical pressure response when backflow is prevalent. Initially the pressure increased as expected until reaching a maximum value; the pressure then exhibited unfamiliar behavior as fluctuations are noted prior to reaching a stable pressure value. The steady state pressure (84.24 mmHg) was lower than expected when infusing into white matter due to backflow. The upper and lower bounds of the apparent hydraulic conductivity in the fiber direction were calculated using the anisotropic tissue model previously described where $K_{\perp}$ was defined as 2.09E-12 and solving the isotropic solution. The tabulated values for $K_{//}$ are found in Table 3-4. The lowest and highest apparent $K_{//}$ across the data sets were 2.31E-12 and 6.48E-11 $m^4 N^{-1} s^{-1}$. Coronal slices of the final infusate distribution in the internal capsule are presented in Figure 3-8, where the images progress in the posterior direction.

Dynamic Contrast Enhanced MRI Data

During infusion of Evans Blue Gd-Albumin, T1-weighted spin-echo images were repeated acquired to capture the evolution of the contrast agent distribution. Each image generated required a scan time of approximately 3.5 minutes. The infusion pressure was simultaneously recorded and is presented in Figure 3-9. The time intervals for each scan are labeled such that the labeled images in Figure 3-10 and 3-11 correspond to the labeled time intervals in Figure 3-19. Thus, the dynamic pressure and infusate distribution throughout infusion provides correlations between pressure responses and local tissue responses to infusion. The infusate was not visible in the MR images until scans D and C for the dorsal and ventral hippocampus, respectively. These time points correspond to the beginning of pressure stabilization.

Table 3-1. Average steady state pressure during water infusion.

Trial	Pressure (mmHg)	Standard Deviation (mmHg)
1	52.43	0.64
2	51.57	0.59
3	51.66	0.77
4	51.62	0.76
5	52.47	0.65
6	53.11	0.63

Table 3-2. Average steady state infusion pressure and apparent hydraulic conductivity of 2% hydrogel.

Trial	Pressure (mmHg)	Standard Deviation (mmHg)	Apparent Hydraulic Conductivity, K ($m^4 N^{-1} s^{-1}$)
1	102.27	1.61	2.98E-12 ± 9.27E-14
2	103.99	6.90	2.88E-12 ± 3.38E-13
3	85.15	4.08	4.52E-12 ± 4.97E-13
4	80.27	2.44	5.30E-12 ± 4.24E-13
5	99.77	1.57	3.13E-12 ± 1.00E-13
6	105.06	2.06	2.82E-12 ± 1.06E-13

Table 3-3. Average steady state infusion pressure and apparent hydraulic conductivity of rat caudate putamen.

Trial	Pressure (mmHg)	Standard Deviation (mmHg)	Apparent Hydraulic Conductivity, K ($m^4 N^{-1} s^{-1}$)
1	105.02	0.66	2.82E-12 ± 6.74E-14
2	117.03	6.29	2.30E-12 ± 2.22E-13
3	137.75	2.81	1.74E-12 ± 6.73E-14
4	130.96	1.01	1.89E-12 ± 3.85E-15
5	140.04	3.76	1.70E-12 ± 8.07E-14
6	123.63	1.76	2.09E-12 ± 6.75E-14

Table 3-4. Average steady state infusion pressure and apparent hydraulic conductivity of rat internal capsule.

Trial	Pressure (mmHg)	Standard Deviation (mmHg)	Apparent Hydraulic Conductivity, K ($m^4 N^{-1} s^{-1}$)
1	116.79	0.85	2.31E-12 – 4.85E-11
2	107.55	4.18	2.69E-12 – 5.73E-11
3	110.76	1.53	2.55E-12 – 5.40E-11
4	101.60	0.98	3.02E-12 – 6.48E-11

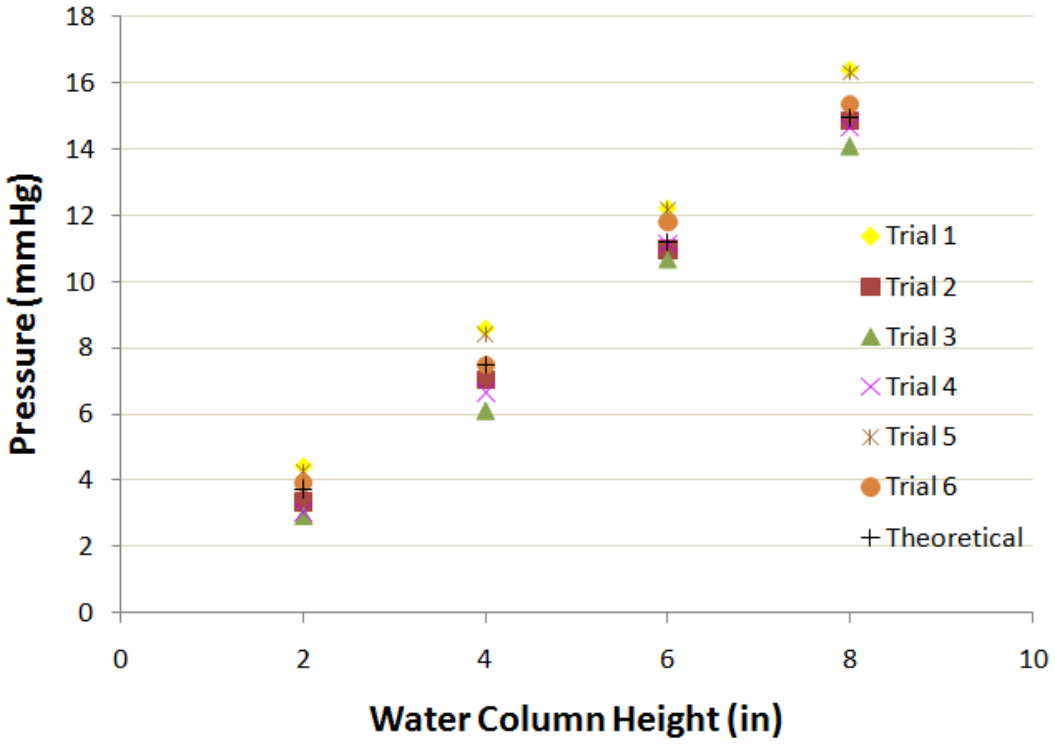

Figure 3-1. Calibration of pressure transducer in column of water.

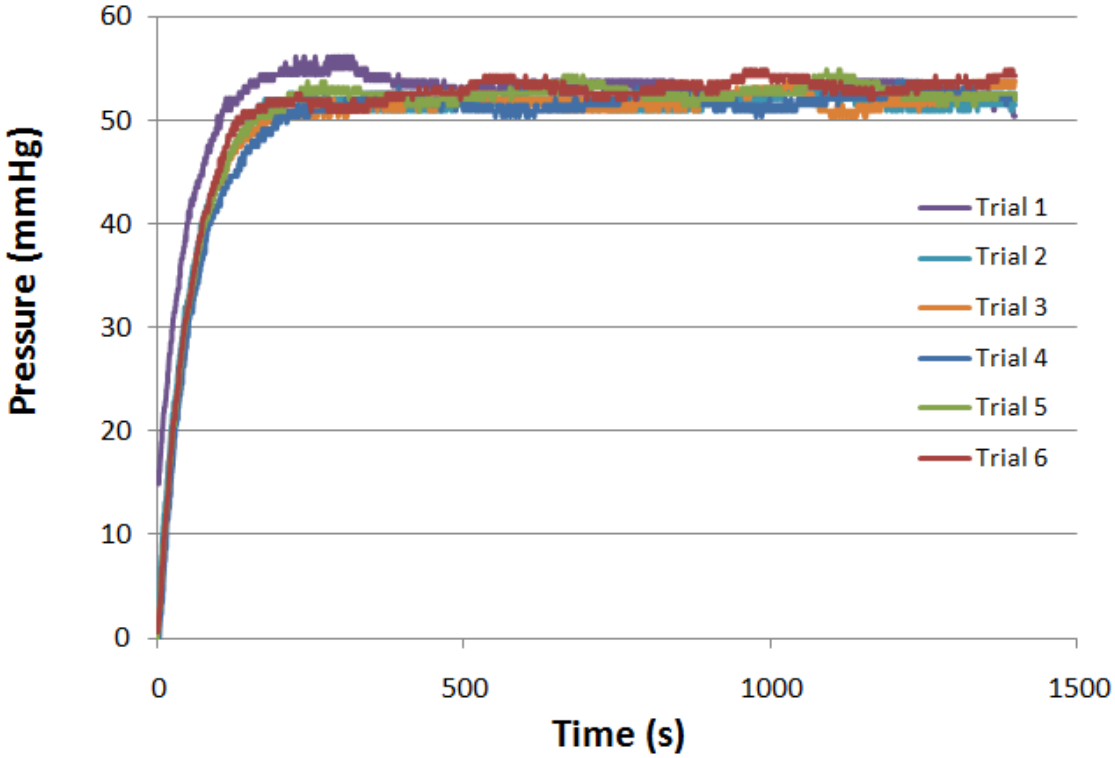

Figure 3-2.Calibration of experimental system by infusion into water.

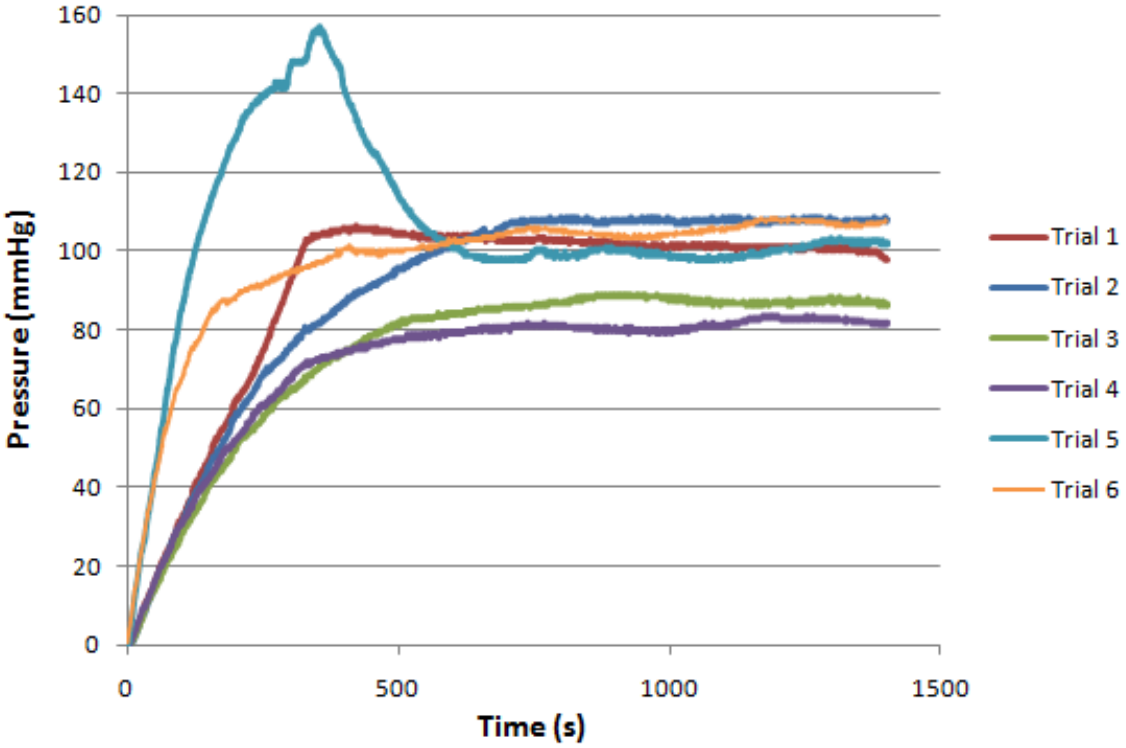

Figure 3-3. Pressure monitoring during infusion into 2% hydrogel (n=6).

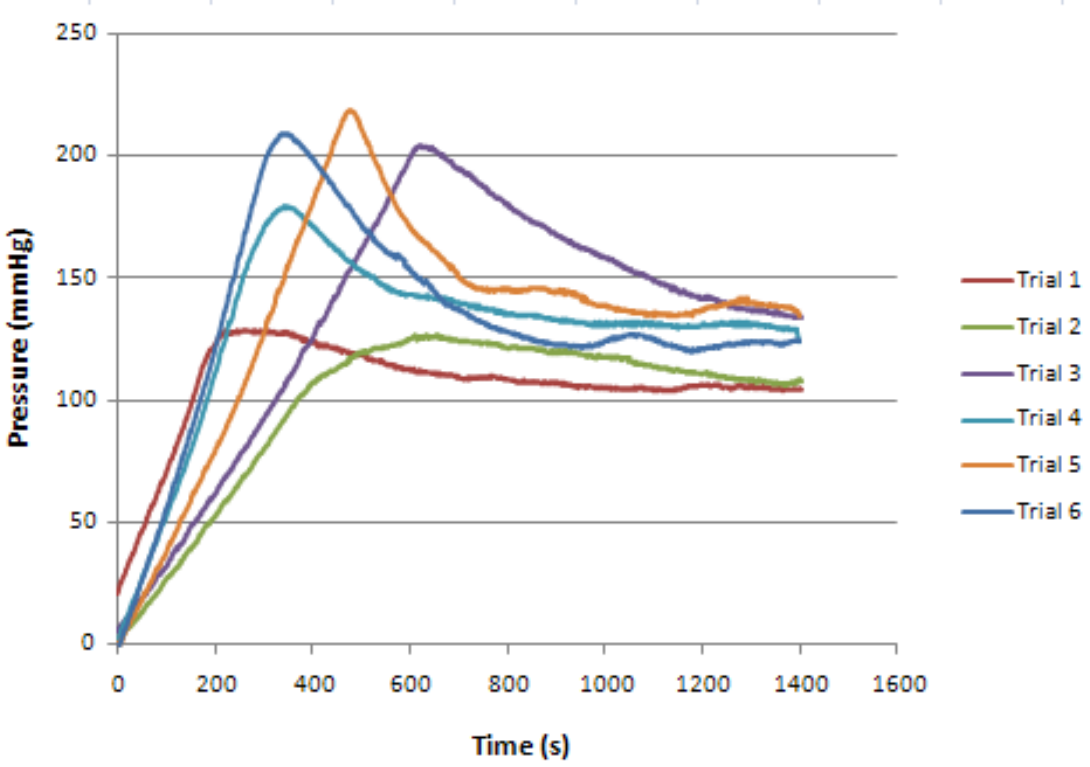

Figure 3-4. Pressure monitoring during infusion into rat caudate putamen (n=6).

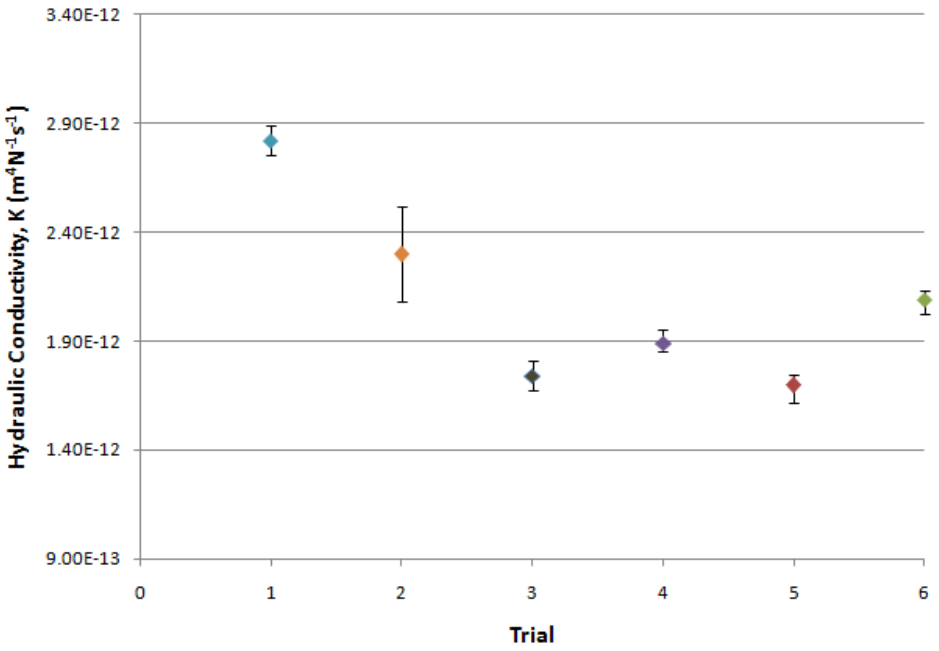

Figure 3-5. Apparent hydraulic conductivity of the rat caudate putamen (n=6).

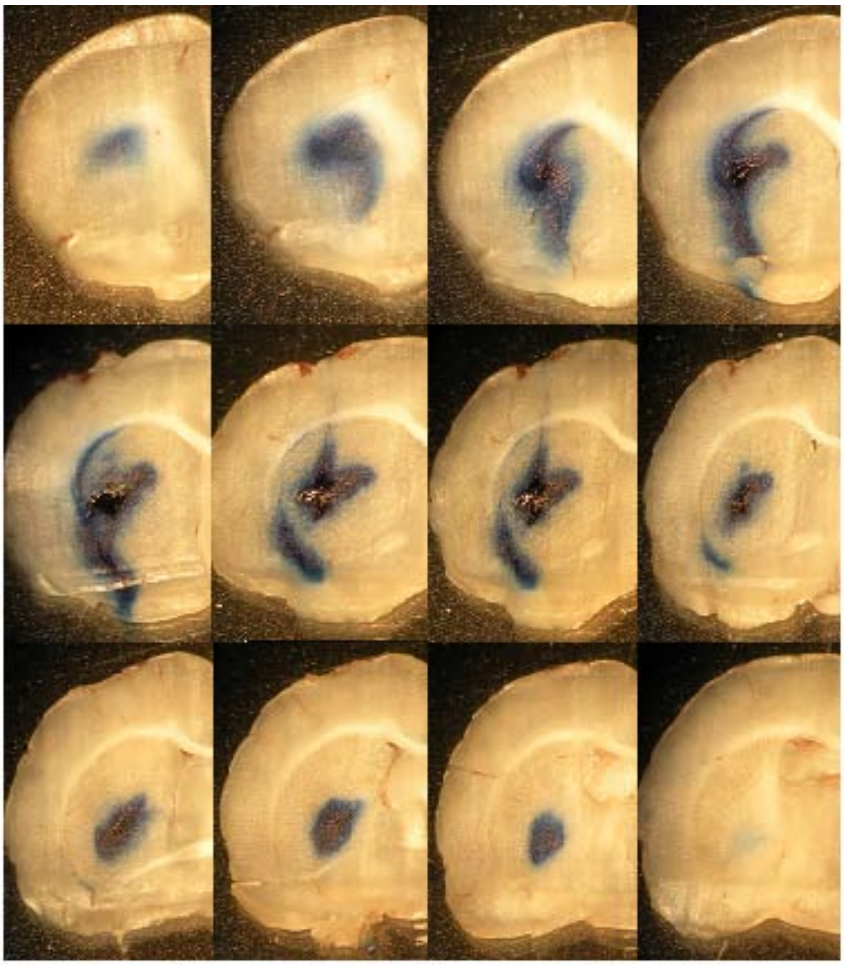

Figure 3-6. Coronal slices (400 um) of rat brain post infusion into the caudate putamen.

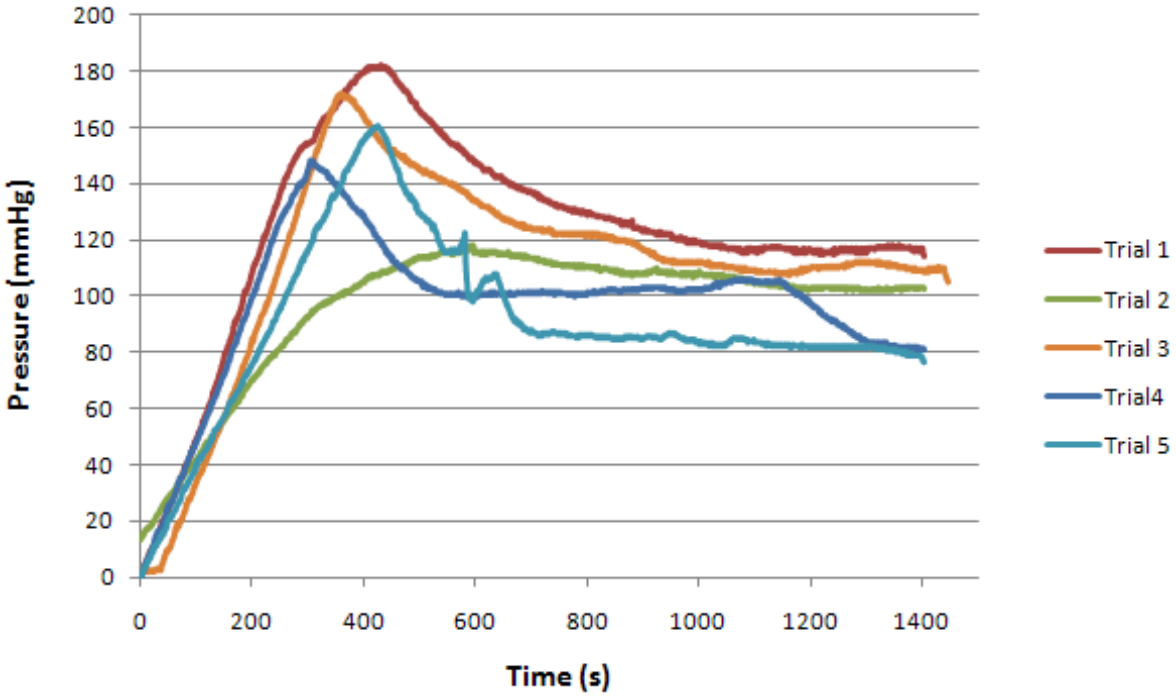

Figure 3-7. Pressure monitoring during infusion into rat internal capsule (n=5).

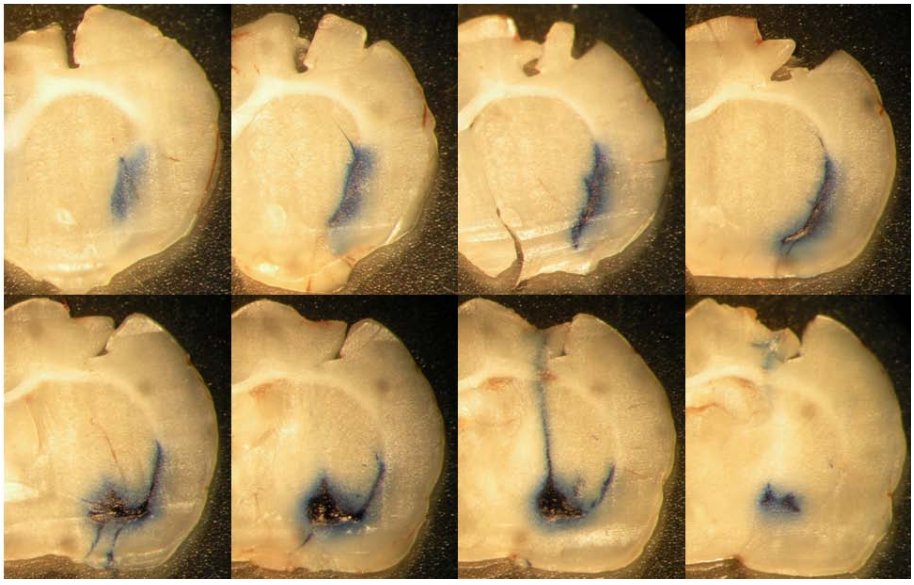

Figure 3-8. Coronal slices (400 um) of rat brain post infusion into the internal capsule.

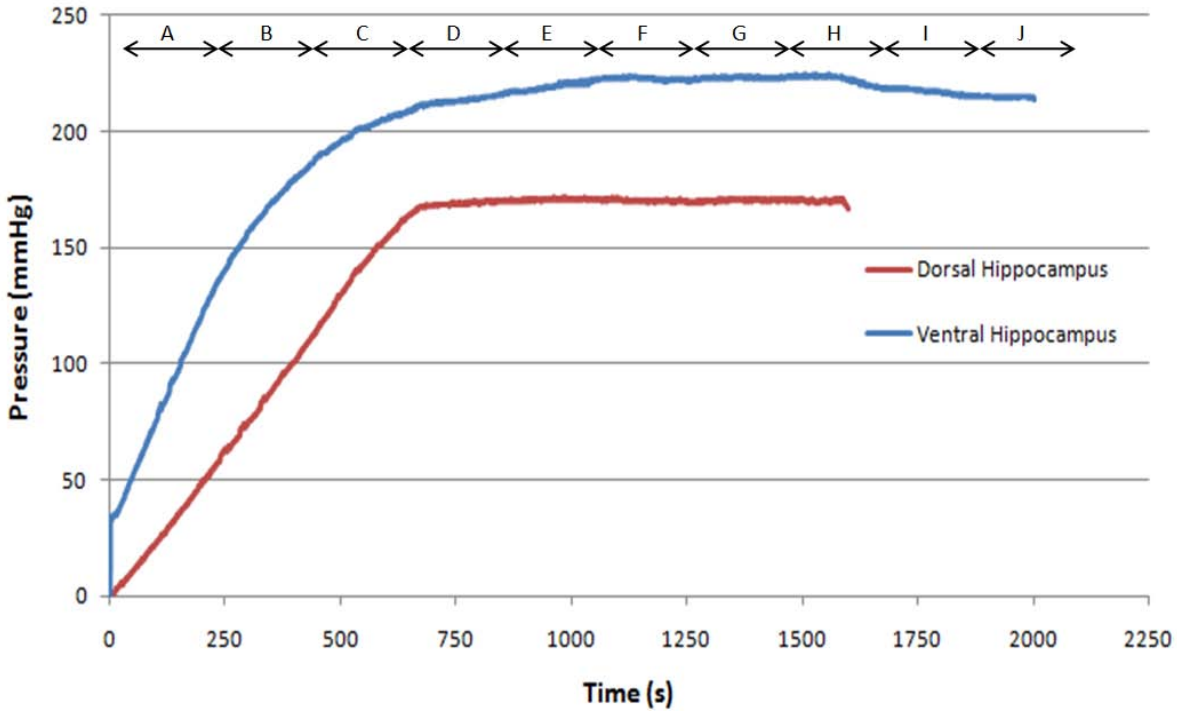

Figure 3-9. Pressure monitoring during infusion into rat dorsal and ventral hippocampus.

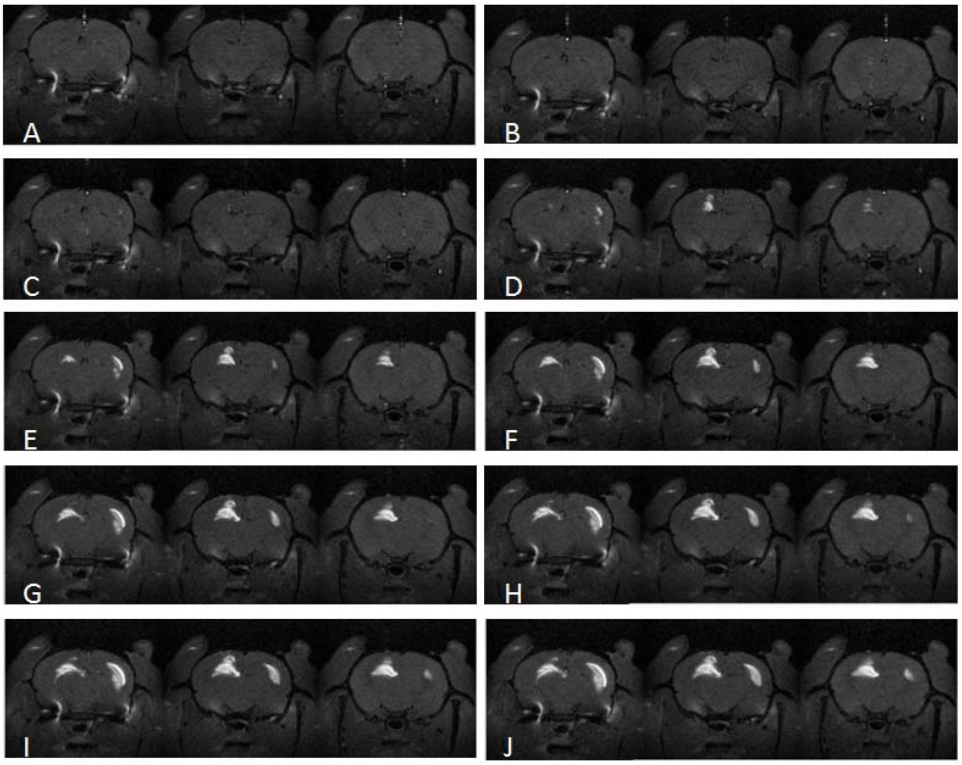

Figure 3-10. MR images of infusate distribution in dorsal hippocampus.

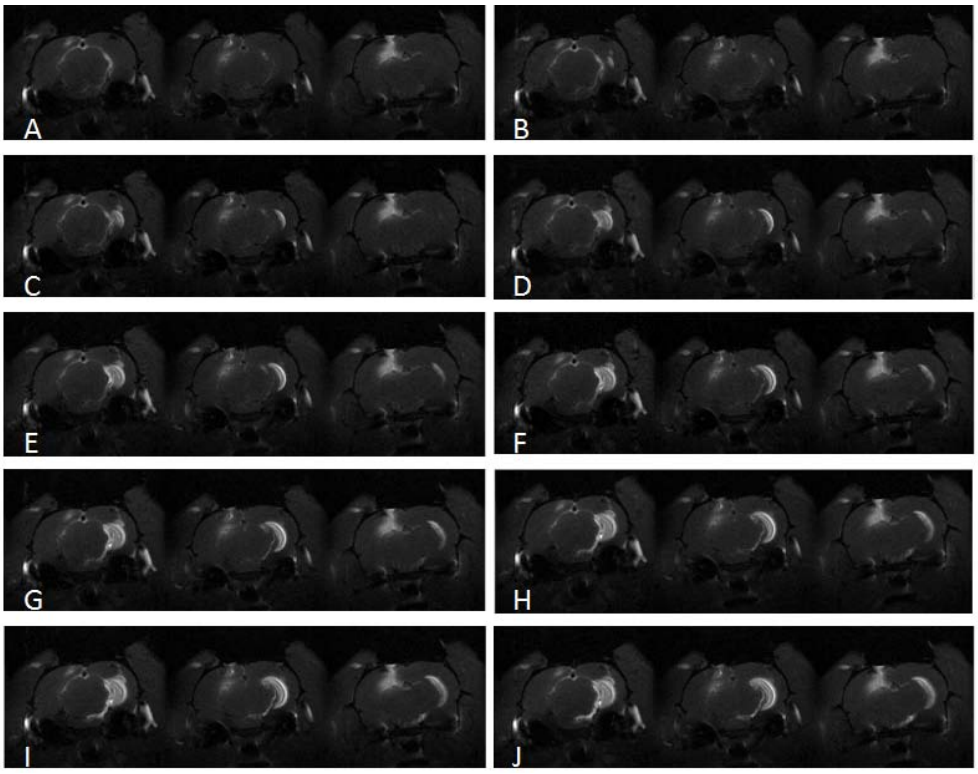

Figure 3-11. MR images of infusate distribution in ventral hippocampus.

CHAPTER 4
DISCUSSION

The developed infusion pressure system described provides useful insight into the characterization of tissue infusions. Drastic increases in infusion pressure followed by a rapid decline indicated the cannula was initially clogged and a bolus injection of infusate was administered once the pressure threshold to release the obstruction was obtained. Cannula retraction was implemented to decrease the likelihood of cannula clogging and backflow as a result of bolus injections. However, retraction was only found to be effective when a five to ten minute wait period occurred between cannula placement and infusion. It is hypothesized that this effect is due to tissue relaxation. The pressure monitoring system provided knowledge as to the severity of backflow. In extreme cases, where backflow became evident on the surface of the brain, the infusion pressure reached extremely low values. In less severe cases, the infusion pressure was found to be low and/or characterized by variance or lack of pressure stabilization.

The average apparent hydraulic conductivity of 2% hydrogel (3.61E-12 ± 3.38E-13 $m^4 N^{-1} s^{-1}$) was found to be greater than previously published values. These differences can be explained by the methods used to derive the apparent hydraulic conductivity and the various hydrogel preparation procedures used. Gu et al exposed hydrogel samples to 10% compressive strain and obtained an average value of 6.61E-13 $m^4 N^{-1} s^{-1}$ for 2% hydrogel. Johnson and Deen forced infiltrate through hydrogel samples at a constant pressure of 20 kPa. These studies provide hydraulic conductivity values across a bulk sample while the goal of our study was to determine local hydraulic conductivity of tissue during infusion. Thus, an increase in permeability with respect to infusion pressure is expected in radial flow experiments irrespective of the porous media under

investigation (Zhang, X 2000). Neeves et al used a micro-fluidic probe to infuse into 0.6% hydrogel samples at constant pressures of 7, 35, 70, 140, 210 and 310 kPa. The average apparent hydraulic conductivity reported in their study was 2.05E-12 $m^4N^{-1}s^{-1}$. However, the average infusion pressure in our study was 5.9 ± 1.4 kPa which is at least one order of magnitude lower than those of the previously mentioned studies. As expected, the lower infusion pressure values yielded apparent hydraulic conductivities one order of magnitude larger than those of the aforementioned studies.

The gray and white matter infusion studies yielded apparent hydraulic conductivities in accordance with previously published values, 2.09E-12 and 2.31E-12 to 6.48E-11 $m^4N^{-1}s^{-1}$, respectively. Neeves et al reported an apparent hydraulic conductivity of 5E-12 $m^4N^{-1}s^{-1}$. Although, the hydraulic conductivity in the transverse direction is unknown for white matter; a range encompassing the upper and lower limits of this value was used to calculate a range of values for the apparent hydraulic conductivity in the fiber direction. Using unconfined compression techniques on excised calf brains, Cheng et al applied a poroviscoelastic model to determine the hydraulic permeability of white matter and reported it to be on the order of 10^{-12} $m^4N^{-1}s^{-1}$. This study differs drastically from their study as different animal brain tissues were used (rat versus calf; internal capsule versus corpus callosum; *in vivo* versus excised), the methods used to model the tissue also varied (rigid versus poroviscoelastic) and the experimental conditions also differed (infusion vs. unconfined compression). These differences account for the discrepancies between the values obtained. No previous studies have determined the hydraulic permeability of white matter via infusion techniques. However, it is known that in white matter preferential flow exists along the

fiber direction; thus, lower infusion pressures and larger hydraulic conductivity values along the fiber direction were expected. Thus, the range of values obtained for $K_{//}$ can be used in transport models to better quantify infusion distributions in white matter structures.

In the MR studies, the pressure data provided a quantitative understanding of infusion in tissue while the MR images provided visual insight into the tissue response throughout infusion. When coupled, investigators have a complete understanding of what is occurring locally in the tissue throughout infusions. Both methods worked hand-in-hand to explain what was physically occurring in the tissue throughout the infusion and this characterization allowed for a more thorough and comprehensive investigation of infusions.

Pressure due to constant flow rate infusion is highly dependent on the tissue hydraulic conductivity as expressed in Equation 1-3. High pressure and stress may cause necrosis or apoptosis to occur near the infusion site (Morrison, B. 2000). Thus, the infusion pressure monitoring system described is useful in preventing the tissue from exposure to large stresses and deformations which could result in cell death. The system also provides clinicians with an easy to use and cost effective method of monitoring infusions in situations where critical care must be taken throughout treatment due to the delicate nature of the disease, patient condition and/or the high accuracy required for administering medications in certain regions of the body. Computational transport models could also benefit from more accurate characterization of tissue properties and the infusion pressure system is capable of defining the apparent hydraulic conductivity of soft biological tissues.

LIST OF REFERENCES

Barry S, Aldis G. Flow-Induced Deformation from Pressure Cavities in Absorbing Porous Tissues. Bull Math Biol 1992; 54: 977-97.

Basser PJ. Interstitial Pressure, Volume, and Flow during Infusion into Brain Tissue. Microvasc Re. 1992; 44: 143-65.

Bidros D, Vogelbaum M. Novel Drug Delivery Strategies in Neuro-Oncology. Neurotherapeutics 2009; 6: 539-46.

Bobo RH, Laske DW, Akbasak A, Morrison PF, Dedrick, RL, Oldfield, EH. Convection-enhanced delivery of macromolecules in the brain. Proc Natl Acad Sci 1994; 91: 2076-80.

Boucher Y, Baxter LT, Jain RK. Interstitial Pressure Gradients in Tissue-isolated and Subcutaneous tumors: Implications for therapy. Cancer Res 1990; 50: 4478-84.

Boucher Y, Brekken C, Netti PA, Baxter LT, Jain RK. Intratumoral infusion of fluid: Estimation of hydraulic conductivity and implications for the delivery of therapeutic agents. Br J Cancer 1998; 78: 1442-48.

Chen MY, Lonser RR, Morrison PF, Governale LS, Oldfield EH. Variables affecting convection-enhanced delivery to the striatum: a systematic examination of rate of infusion, cannula size, infusate concentration and tissue-cannula sealing time. J Neurosurg 1999; 90: 315-20.

Cheng S, Bilston L. Unconfined compression of white matter. J Biomech 2007; 40: 117-24.

Cunningham J, Pivirotto P, Bringas J, Suzuki B, Vijay S, Sanftner L, et al. Biodistribution of adeno-associated virus type-2 in nonhuman primates after convection-enhanced delivery to brain. Mol Ther 2008; 16:1267-75.

Gu WY, Mao XG, Foster RJ, Weidenbaum M, Mow VC, Rawlins BA. The Anisotropic Hydraulic Permeability of Human Lumbar Anulus Fibrosus: Influence of Age, Degeneration, Direction and Water Content. Spine 1999; 24: 2449-55.

Gu WY, Yao H, Huang CY, Cheung HS. New insight into deformation-dependent hydraulic permeability of gels and cartilage, and dynamic behavior of agarose gels in confined compression. J Biomech 2003; 36: 593-98.

Johnson E, Deen W. Hydraulic Permeability of Agarose Gels. AIChE J 1996; 42: 1220-24.

Kim JH, Astary GW, Chen XM, Mareci TH, Sarntinoranont M. Voxelized Model of Interstitial Transport in the Rat Spinal Cord Following Direct Infusion into White Matter. J Biomech Eng 2009; 131:071007-1-8.

Kim JH, Mareci TH, Sarntinoranont M. A voxelized model of direct infusion into the corpus callosum and hippocampus of the rat brain: model development and parameter analysis. Med Biol Eng Comput 2010; 48: 203-14.

Krauze MT, Forsayeth J, Yin D, Bankiewicz, KS. Chapter 18 Convection-Enhanced Delivery of Liposomes to Primate Brain. Methods in Enzymology 2009; 465: 349-62.

Lee S, Pishko GL, Astary GW, Mareci TH, Sarntioranont M. Characterization of Anisotropic Hydrogel Tissue Substrate for Infusion Testing. J Appl Poly Sci 2009; 114: 1992-2002.

Merritt, HH and Fremont-Smith F (1937) *The Cerebrospinal Fluid*, Philadelphia, PA.
Morrison, B, Eberwine, JH, Meaney, DF, and McIntosh, TK. Traumatic injury induces differential expression of cell death genes in organotypic brain slice cultures determined by complementary DNA array hybridization. Neurosci 96: 131-39.

Morrison PF, Chen MY, Chadwick RS, Lonser RR, Oldfield EH. Focal delivery during direct infusion to brain: role of flow rate, catheter diameter and tissue mechanics. Am J Physiol Regul Integr Comp Physiol 1999; 277: 1218-29.

Neeves KB, Lo CT, Foley CP, Saltzman WM, Olbricht, WL. Fabrication and characterization of microfluidic probes for convection enhanced delivery. J Controlled Release 2006; 111: 252-62.

Pishko GL, Lee SJ, Wanakule P, Sarntinoranont M. Hydraulic permeability of a hydrogel-based contact lens membrane for low flow rates. J Appl Poly Sci 2007; 104: 3730-5.

Prokopova S, Vargova L, Sykova E. Heterogeneous and anisotropic diffusion in the developing rat spinal cord. NeuroReport 1997; 8: 3527-32.

Rapoport SI. Blood-brain barrier. Nature 1980; 283: 414.

Sarntinoranont M, Chen X, Zhao J, Mareci T. Special Delivery Researchers use simulation and medical imaging to explore new options for managing pain. ANSYS Advantage 2007; 1: 13.

Watson S, Gander MJ, MacPherson WN, Barton JS, Jones JDC, Klotzbuecher T, et al. Laser-machined fibers as Fabry-Perot pressure sensors. Appl Opt 2006; 45: 5590-6.

Weiss J, Maakestad B. Permeability of human medial collateral ligament in compression transverse to the collagen fiber direction. J Biomech 2006; 39: 276-83.

Widmaier, E, Raff, H and Strand, KT. *Vander's Human Physiology The Mechanisms of Body Function.* 11th ed. New York: McGraw-Hill (2008). Print.

Zeman, Wolfgang. Craigie's Neuroanatomy of the Rat. New York, NY: Academic Press, 1963. Print.

Zhang XY, Luck J, Dewhirst MW, Yuan F. Interstitial hydraulic conductivity in a fibrosarcoma. Am J Physiol Heart Circ Physiol 2000; 279: H2726-34.

BIOGRAPHICAL SKETCH

Tatiana Lopez Nobrega was born in Rochester, NY. She graduated high school from Felix Varela Senior High in Miami, FL and attended the University of Florida. She graduated summa cum laude from the University of Florida in May 2009 with a Bachelor of Science in mechanical engineering and a minor in biomechanics. Tatiana will graduate in December of 2010 with a Master of Engineering in biomedical engineering.